VENTILATED FLAT ROOFS: A SIMPLIFIED MODEL TO ASSESS THEIR HYGROTHERMAL BEHAVIOUR

Francesco Leccese [a,*], Giacomo Salvadori [a], Maksym Barlit [b]

[a] University of Pisa, School of Engineering, Largo Lucio Lazzarino, 56122, Pisa, Italy

[b] Laterlite SpA, Via Vittorio Veneto, 43046 Rubbiano (PR), Italy

[*] Corresponding Author: Prof. Francesco Leccese, Largo Lucio Lazzarino 2, 56122 Pisa, Italy
Tel. +39 (0)50.2217.158, e-mail: f.leccese@ing.unipi.it

Abstract

The hygrothermal behaviour of the opaque building envelope (facades and roofs) is a topic worthy of investigation for the scientific community, especially in consideration of changes in construction techniques and lifestyle habits. For the presence of waterproofing layers, placed in the outer part of a structure, hygrothermal behaviour of flat roofs is of particular interest. In this paper, an original analytical model for evaluation of the hygrothermal behaviour of ventilated flat roofs is proposed. In particular, the authors provide a method for assessing the ventilation air flow rates necessary to avoid interstitial condensation in flat roofs. Dependency of the necessary ventilation air flow rates on geometrical, thermophysical, and climate parameters is investigated and discussed. After a simplified analytical treatment applicable to any type of ventilated flat roof, some examples are shown, referred to study cases of flat roofs that are very widespread in Italy. The results obtained by the authors and discussed in the paper can be useful for architects and building engineers during the early design stage of buildings.

Keywords: ventilated roof; flat roof; hygrothermal behaviour; interstitial condensation; analytical model.

1- Introduction

The hygrothermal behaviour of the opaque building envelope (facades and roofs) has been the subject of numerous studies [1-5] and of some technical standards [6,7], with the main aim to analyse both surface and interstitial condensation phenomena, also within the implementation of the acknowledgment Decrees for the European Energy Performance of Buildings Directives [8,9].

At European level, the standard EN ISO 13788 [6] describes a simplified method, which can be used to assess the risk of internal surface condensation and also to assess the risk of interstitial condensation due to water vapour diffusion, is discussed. The method is based on steady-state heat and mass transfer conditions and, in the case of interstitial condensation that evaporates during the summer season, it allows the determination of the time taken for water to dry out. The standard EN

15026 [7] specifies a set of equations, to be used in a simulation method for calculating the unsteady-state heat and moisture transfer through the building structures. Moreover a benchmark example, intended to be used for validating the simulation method claiming conformity with this standard, is also indicated together with the allowed tolerances. Both the aforesaid methods, steady-state and unsteady-state [6,7], do not allow to consider the effects of ventilated air gaps.

In Italy, in the recent Decree of June 2015 [10] on the minimum energy efficiency requirements for buildings, it is indicates that the opaque envelope structures, for new buildings and buildings under renovation, must be free of both internal surface and interstitial condensation risks. This requirement is more restrictive than the one contained in the Italian legislation previously in force [11], which permitted the possibility of formation of the interstitial condensation, providing that it was limited and completely re-evaporable throughout the summer season. The requirement could appear strongly restrictive, especially in light of the calculation method [6] suggested by the Decree. The suggested method [6] tends to overestimate the risk of interstitial condensation, neglecting some phenomena that affect the building structures, e.g. capillarity and hygroscopic capacity of the materials. This attitude, anyway, shows an increasing attention to the condensation risk in building structures, also related to changes in lifestyle habits and in constructive techniques [12,13]. At the same time this attitude shows a need to provide designers with simplified tools for an early evaluation of design solutions, referring to more in-depth assessments where necessary.

The risk of surface condensation mainly depends on the temperature of the inner face of the building structure and on the indoor air conditions (temperature and relative humidity). As a consequence this risk (as well as the risk of mould growth) can be avoided, both for traditional and for innovative envelopes, giving an adequate level of thermal insulation to the analysed building structures in function of the indoor air conditions [14,15]. The risk of the interstitial condensation strongly depends on the order of succession of the layers that make up the building structure, in this regard very particular is the hygrothermal behaviour of both tilted and flat roofs. More specifically, in the tilted roofs condensation occurs only rarely, since it is often possible to dispose of the moisture generated in the rooms by means of air ventilation [16] of the environments underlying the roof (attics or crawl spaces) that are generally not inhabited. In the case of habitable attic, if the roof covering is realized with terracotta tiles (widespread in Europe) [17], between the covering and the underlying bearing structure a micro-ventilation is activated [18-20], which in many cases is sufficient to prevent condensation phenomena. In flat roofs, the presence of the waterproofing layer [21], placed in a disadvantageous position by the hygrothermal point of view, often results in considerable condensation phenomena during the winter and prevents the evaporation of the condensate during the summer. The formation of the interstitial condensation can be avoided by the application of a vapour barrier, but this solution must be considered with extreme caution for the issues it can cause [22], which sometimes can undo the advantages that would be achieved with its use. In these cases, to avoid interstitial condensation may be a convenient solution to introduce ventilated air gaps [23,24].

Ventilation of tilted roofs usually occurs naturally by means of chimney effect [25-27], on the contrary in the case of flat roofs (subject of this work) or with very small tilt angles (generally less than 3°, made exclusively for proper disposal of the rainfall), forced ventilation must be used.

In the scientific literature, considerable attention has been paid to the study of the walls and tilted roofs with ventilated air gap, especially from the point of view of energy performance [28-30], both through numerical models [31-35] and experimental analysis [36-39]. Focusing the discussion on the numerical models, Ciampi et al. [20,27] developed an interesting analytical model for naturally ventilated roofs, aimed to predict the convenience of using ventilated roofs for the reduction of summer thermal loads, introducing an original parameter to evaluate the energy saving potential. The analysis was carried out both in case of turbulent flow and laminar flow (micro-ventilation) within the air duct. Tong and Li [37] used an analytical approach, based on the electrical analogy, to develop an efficient model for the prediction of the heat flux transferred through the naturally ventilated roofs. The model was validated by comparison with CFD analysis results and experimental results. More recently, Bortoloni et al. [18], Gagliano et al. [26], Li et al. [34] used the CFD analysis in order evaluate the summer thermal performance of naturally ventilated roofs, varying different influencing parameters both geometric and climate. All these models are useful for evaluation of the thermal behaviour, but not of the hygrometric one and they refer only to tilted roofs, where natural ventilation is possible.

The hygrothermal behaviours of three different flat roofs was studied by Ghazi Wakili and Frank [39], using numerical and experimental analysis. The numerical analysis was carried out in steady-state and transient conditions by way of the Glaser method [6] and the WUFI simulation software respectively. The results of the numerical analysis were compared with those obtained from long term in-situ measurements. Tian et al. [35] developed an heat and mass transfer model to evaluate the transient hygrothermal behaviour of the green flat roofs. As the thermal conductivity of the soil changes as a function of moisture content, the model was used in order to predict the effective heat flux through the green roof for a high efficient usage and a better application of engineering. These models, applied to flat roofs, consider the thermal and hygrometric effects but are not directly applicable to ventilated roofs.

The literature is lacking in analytical models for predicting the hygrothermal behaviour of flat ventilated roofs, subject matter of this paper. In particular, the authors provide a method for assessing the ventilation air flow rates necessary to avoid interstitial condensation in flat roofs. In the paper a simplified analytical model, applicable to any type of ventilated flat roof, is described and then study cases, referred to different types of flat roofs very widespread in Italy, are reported. The results obtained by the authors and discussed in the paper can be useful for architects and building engineers during the early design stage of buildings.

2- The analytical model

Consider a flat roof having an area S, composed of various layers (the n^{th} of which has thickness d_n) and an air gap through which air flows at a constant flow rate (G). The air gap may be schematically represented as an open system having an inlet vent (1) and an outlet vent (2). The system is involved in an heat transfer (Q_s) with the outdoor environment through the external cladding (s) and in an heat transfer (Q_c) with the indoor environment through the internal cladding (c). Let G_v be the vapour flow rate that comes into the air gap via diffusion through the cladding (c); it is assumed that vapour, in passing through the cladding (c), does not undergo a phase change, in other words, it is assumed that in each point within (c) the water vapour pressure is always less than the saturated vapour pressure at the same temperature. In the cladding (s) there is a waterproof layer (b) which acts as a vapour barrier. A simple schematization of the ventilated flat roof under examination is shown in Figure 1.

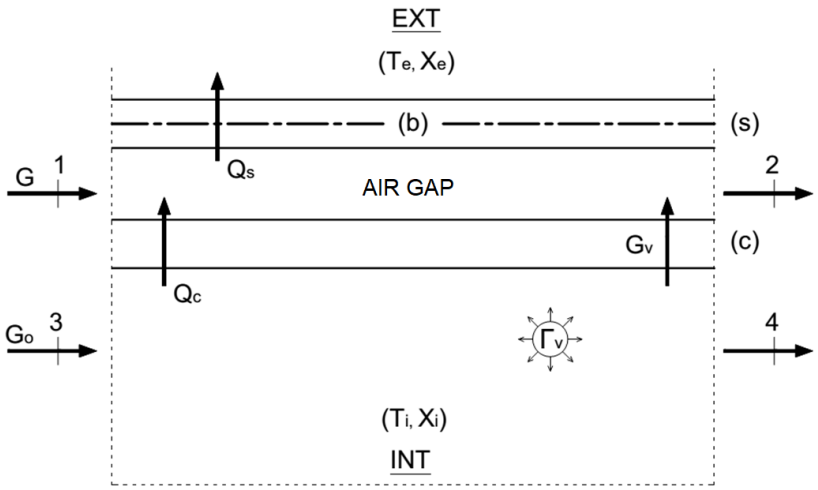

Figure 1: Schematization of the analysed ventilated flat roof (in the figure the symbol INT represents the indoor environment and the symbol EXT represents the outdoor environment).

Let T_e, X_e, I_e be the temperature, the humidity ratio and the enthalpy of external air; T, X, I are the corresponding values relative to the mean air gap conditions. Within the room, of volume V, there is a heating system which maintains a mean temperature T_i; furthermore, G_0 is the air flow rate into the room through section 3 and out of the room through section 4, Γ_v is the internal moisture production rate (per unit area of the roof) and X_i the humidity ratio of internal air. The heat transfer due to solar radiation is not considered. The heat flux is assumed to be unidimensional, so that any effects caused by thermal bridges are disregarded. All flow rates are expressed, unless otherwise specified, as mass per unit area of the roof. For the air gap, in steady state conditions, the following equations can be posed:

$$G\,(I_2 - I_1) = Q_c - Q_s \quad (1)$$

$$G\,(X_2 - X_1) = G_v \quad (2)$$

having indicated with X_1 and I_1 the humidity ratio and enthalpy of moist air at the inlet vent and with X_2 e I_2 the corresponding values at the outlet vent. Obviously: $X_1=X_e$ and $I_1=I_e$; hereafter it will be assumed that hygrothermal conditions of air at the outlet vent are coincident with the mean ones in the air gap, such that: $X_2=X$ and $I_2=I$. With these assumptions, it follows that:

$$Q_c=(T_i - T)R_c^{-1} \quad \text{and} \quad Q_s=(T - T_e)R_s^{-1} \tag{3}$$

with R_c and R_s thermal resistances between air in the air gap and air in the indoor and outdoor environments respectively. These thermal resistances can be calculated according to the methods indicated in the international standards [40] and scientific literature [20,30]. The vapour flow rate G_v can be calculated as:

$$G_v=(p_{vi} - p_v)R_v^{-1} \tag{4}$$

with: p_{vi} water vapour partial pressure in the room; p_v mean value of water vapour pressure in the air gap; R_v water vapour diffusion resistance of the cladding (c), where $R_v=\sum_{n=1}^{N} d_n \delta_n^{-1}$, δ_n being the water vapour permeability of the n^{th} layer. All the thermal and vapour diffusion resistances introduced up to now and hereafter are referred to unit area. The difference in enthalpy in Eq.(1) may be calculated, with a good approximation, using the following relation:

$$I_2 - I_1=c_p(T - T_e)+ r_0(X - X_e) \tag{5}$$

with: c_p specific heat at constant pressure of dry air; r_0 specific latent heat for evaporation of water (at 0°C). For the room, neglecting the vapour flows through all delimiting structures excluding the cladding (c), in the steady state the following equation can be written:

$$G_0(X_4 - X_3)= \Gamma_v - G_v \tag{6}$$

assuming: $X_4=X_i$ and $X_3=X_e$.

Let χ be the ratio between the gas constants for dry air and water vapour, p be the total pressure of moist air and p_{ve} be the water vapour partial pressure of the external air, the followings can be written (excluding second order terms in $p_v p^{-1}$, $p_{vi}p^{-1}$ and $p_{ve}p^{-1}$):

$$X-X_e=\chi(p_v - p_{ve})p^{-1} \quad \text{and} \quad X_i - X_e=\chi(p_{vi} - p_{ve})p^{-1} \tag{7}$$

From Eq.(6), with water vapour partial pressure $\bar{p}_{vi}$ defined as:

$$\bar{p}_{vi}=p_{ve}+p\Gamma_v(\chi G_0)^{-1} \tag{8}$$

and using Eqs.(4) and the second of Eqs.(7), it follows that:

$$p_{vi} - p_v=\frac{1}{1+gG_0^{-1}}(\bar{p}_{vi} - p_v) \tag{9}$$

with $g=p(\chi R_v)^{-1}$.

From Eq.(2), using Eqs.(4), (9) and the first of Eqs.(7), it can be obtained:

$$G=\frac{g}{1+gG_0^{-1}}\left(\frac{\bar{p}_{vi}-p_v}{p_v-p_{ve}}\right) \tag{10}$$

which expresses the air flow rate in the air gap as a function of given quantities (which are to be considered as input data) and pressure p_v. In many practical cases $gG_0^{-1}<<1$, so that the multiplying coefficient in Eq.(10) may be approximated by g and from Eq.(9) can be obtained: $\bar{p}_{vi} \cong p_{vi}$.

The air temperature (T) in the air gap is easily obtained from Eq.(1) using Eqs.(3), (5) and the first of Eqs.(7):

$$T = T_e + \frac{1}{1+\alpha G}\left[\frac{T_i - T_e}{1+\eta} - \alpha G H (p_v - p_{ve})\right] \quad (11)$$

having defined:

$$H = r_0 \chi (p c_p)^{-1} \quad , \quad \alpha = R_p c_p \quad , \quad \eta = R_c R_s^{-1}$$

with: $R_p^{-1} = R_c^{-1} + R_s^{-1}$

From Eq.(11), with G=0, it follows:

$$T = T_0 = \frac{R_s T_i + R_c T_e}{R_s + R_c}$$

which represents the air temperature in the air gap in the absence of ventilation.

To avoid interstitial condensation phenomena in the roof, the water vapour partial pressure in the air gap must be less than the saturated vapour pressure p_s at the temperature T_b of the waterproofing layer, expressed by:

$$T_b = T - \beta (T - T_e) \quad (12)$$

with: $\beta = R_0 R_s^{-1}$; R_0 thermal resistance between air in the air gap and the lower face of waterproofing layer. The ventilation air flow rate G, needed for avoiding condensation, may be calculated using the following condition:

$$p_v = p_s \quad (13)$$

which implies a limit for the waterproofing layer temperature as it cannot fall below the value (T_b) implicitly set by Eq.(13).

In the special case of a non-ventilated air gap (G=0), clearly G_v=0 and p_v=p_{vi}. In such a case, in order to avoid condensation phenomena, it is necessary to set p_{vi}=p_s at the temperature T_b, with T_b given by Eq.(12). From Eq.(6), with the second equation of Eqs.(7), or, simply from Eq.(8) with: $\bar{p}_{vi} = p_{vi}$, the following relation thus follows:

$$G_0^* = \frac{\Gamma_v}{\chi} \frac{p}{p_s - p_{ve}} \quad (14)$$

which can also be obtained from Eq.(10) in the limit case: G=0. The value G_0^*, calculated with Eq.(14), represents the indoor ventilation air flow rate needed to avoid interstitial condensation in a non-ventilated roof.

In general the problem can be solved using the Eqs.(10), (11), (12), (13) and the variables: T, G, p_v and T_b, according to the hygrothermal characteristics of the roof through the parameters: α, β, η and g and according to the boundary conditions: T_i, T_e, Γ_v, G_0 and p_{ve} (which are usually known).

The heat flux (Q) lost through the non-ventilated roof is clearly given by:

$$Q = (T_i - T_e) R_T^{-1} \quad (15)$$

with R_T thermal resistance of the roof including the appropriate term related to the air gap (R_{ca}). The presence of ventilation causes an increment (Δ) in thermal loss given by:

$$\Delta = (Q_c - Q)Q_c^{-1} \quad (16)$$

with Q_c given by the first equation of Eqs.(3).

The Eqs.(10), (11), (12), and (13) can be easily solved using an iterative procedure. For the sake of simplicity, assuming constant the surface thermal resistances of the air gap, it is possible to proceed as indicated in the flow chart shown in Figure 2.

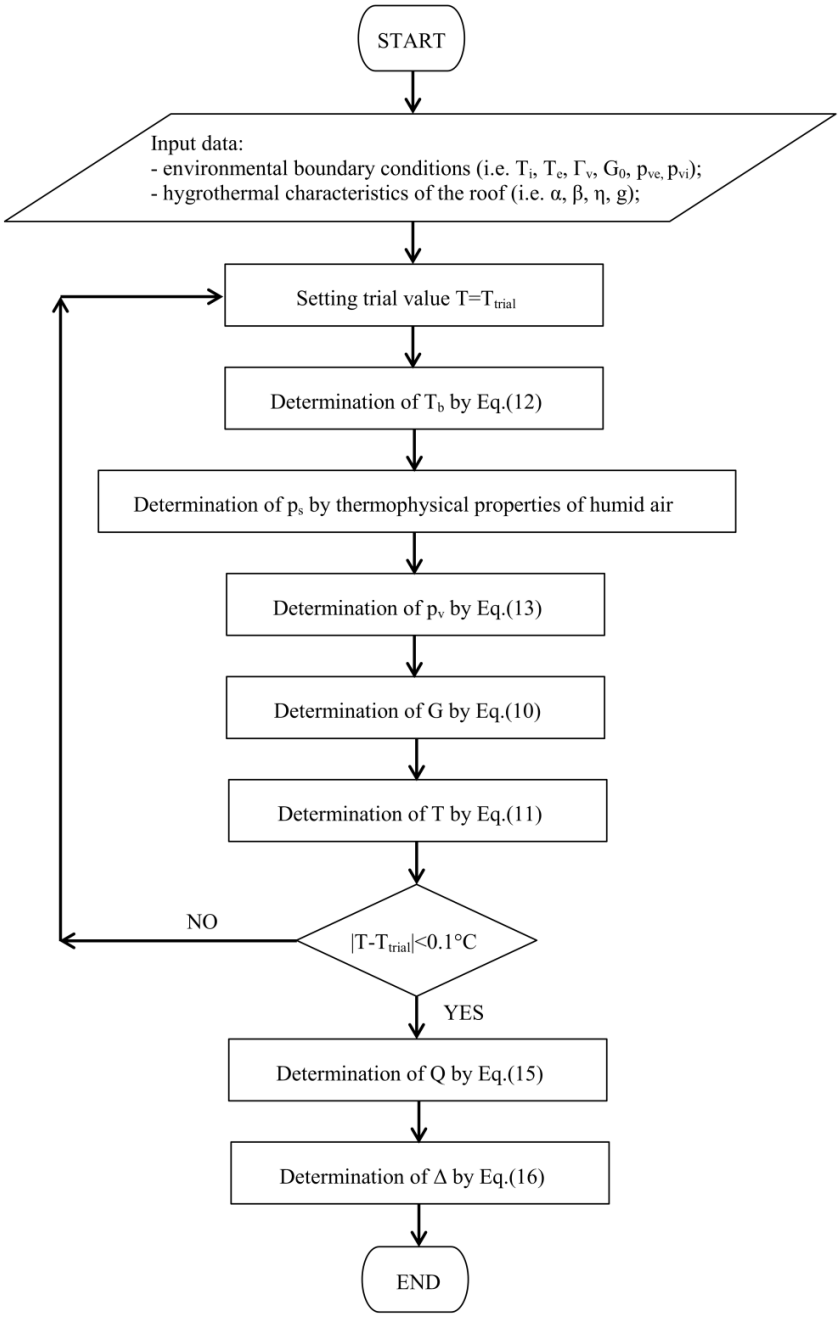

Figure 2: Flow chart for the simplified model implementation.

3- Application of the proposed model to technological solutions

As study cases two flat roofs with a load bearing structures made of concrete beams (in-situ filled) and brick blocks, very widespread in Italy, have been considered. They are characterized by the same overall thickness and by the same overall thermal resistance. This choice depends on the technical interest in the evaluation of the hygrothermal behaviour of solutions with the same overall thickness and the same thermal resistance, as usually happens during the early design stage, rather than solutions with the same R_v (which have the same behaviour according to the proposed analytical model, see e.g. Eq.10).

The R1 roof (see Fig.3) is particularly widespread in multi-storey residential buildings. It represents a common services area and it allows the access for the maintenance of HVAC systems. It has a surface mass of 370 kg/m^2 and it is characterized by the positioning of the load bearing structure (layer 4, Fig.3-left) in the external cladding (s). The R2 roof (see Fig.3) is mainly used in office or commercial buildings and in school buildings. In this structure the false ceiling is generally used to hide the building services (e.g. plant piping, electrical equipment), to host recessed devices (e.g. luminaires, speaker grills) and to aid the room acoustics. It has a surface mass of 280 kg/m^2 and it is characterized by the positioning of the load bearing structure (layer 6, Fig.3-right) in the internal cladding (c).

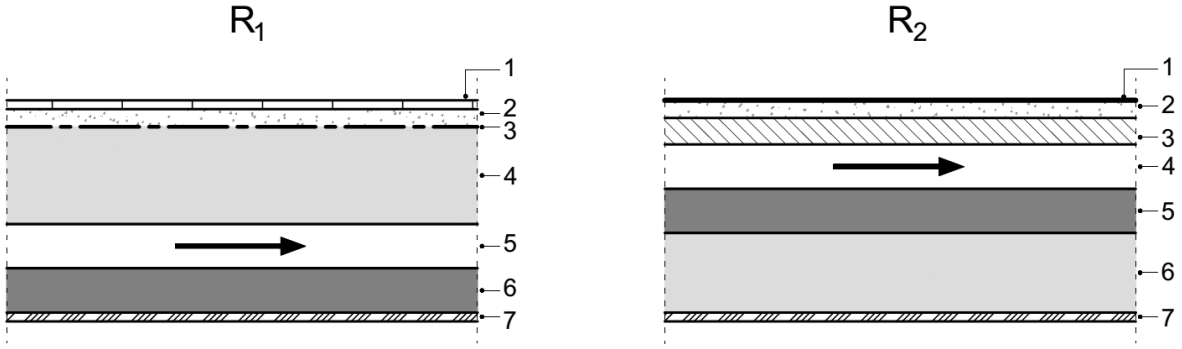

Figure 3: Schematization of the analysed roofs. **R1 roof (left):** (1) flooring, (2) screed, (3) waterproofing layer, (4) concrete beams/brick blocks slab, (5) air gap, (6) thermal insulation, (7) plasterboard. **R2 roof (right):** (1) waterproofing layer, (2) screed, (3) hollow flat tiles, (4) air gap, (5) thermal insulation, (6) concrete beams/brick blocks slab, (7) gypsum plaster.

In Table 1 the main geometric and thermophysical properties of the layers making up the two analysed roofs are shown: thickness d (cm); thermal conductivity k (W/mK); thermal resistance R (m²K/W); water vapour resistance factor μ; equivalent air layer thickness s_d (m), with $s_d=\mu\, d$; water vapor diffusion resistance r_v (m^{2}sPa/kg). The overall thermal resistance (R_T) of the analysed roofs, having a total thickness (d_T) equal to 0.52 m, is 4.0 m^{2}K/W (thermal transmittance U=0.25 W/m^{2}K). The values of R_T were calculated assuming the following thermal resistances [40]: R_{ca}=0.16 m^{2}K/W (closed air gap), R_{si}=0.10 m^{2}K/W (internal surface) and R_{se}=0.04 m^{2}K/W (external surface). The overall water vapour diffusion resistances are: $R_{vT,1}=32.9\times10^{10}$ m^{2}sPa/kg (internal cladding,

$R_{v,1}$=0.16×10^{10} m^2sPa/kg) for R1 roof and $R_{vT,2}$=31.7×10^{10} m^2sPa/kg (internal cladding, $R_{v,2}$=1.49×10^{10} m^2sPa/kg) for R2 roof.

The calculations were carried out for three significant Italian sites, representative of the Italian climate zones (see Annex A): Agrigento (climate zone C), Pisa (D) and Milano (E). For these sites, in Table 2 are shown the monthly mean values of the temperature (T_e), the water vapour pressure (p_{ve}) and the relative humidity (Ψ_e) of the external air, in the case of the 'critical month' (see Annex A). For the external air temperature (see Tab.2), the monthly mean values indicated in [42] have been modified, using the methodology given in [41,43], in order to take into account the cooling effect due to long wave radiation, as suggested also in [6]. This methodology consists in reducing the effective temperature of the external air, up to a value such as to obtain an equivalent thermal flow that includes both the transmission heat loss through the opaque envelope structure and the infrared radiation heat loss towards the sky [6].

Table 1: Thermophysical properties of the analysed roofs.

Roof		Layer	Description	d (cm)	k (W/mK)	r (m^2K/W)	μ	s_d (m)	r_v (m^2sPa/kg)
R1	External cladding (s)	1	[EXT] Flooring	1	1	0.01	200	2	1.00 ×10^{10}
		2	Screed	4	0.58	0.07	1	0.04	0.02 ×10^{10}
		3	Waterproofing layer	0.3	0.17	0.02	20000	60	30.0 ×10^{10}
		4	Concrete beams/brick blocks	22	0.667	0.33	15	3.3	1.65 ×10^{10}
		5	Air gap	10	-	-	-	-	-
	Internal cladding (c)	6	Thermal insulation	12	0.038	3.16	1	0.12	0.06 ×10^{10}
		7	[INT] Plasterboard	2.5	0.21	0.12	8	0.2	0.10 ×10^{10}
R2	External cladding (s)	1	[EXT] Waterproofing layer	0.3	0.17	0.02	20000	60	30.0 ×10^{10}
		2	Screed	4	0.58	0.07	1	0.04	0.02 ×10^{10}
		3	Hollow flat tiles	6	0.43	0.14	5	0.3	0.15 ×10^{10}
		4	Air gap	10	-	-	-	-	-
	Internal cladding (c)	5	Thermal insulation	12	0.038	3.16	1	0.12	0.06 ×10^{10}
		6	Concrete beams/brick blocks	18	0.6	0.3	15	2.7	1.35 ×10^{10}
		7	[INT] Gypsum plaster	1.5	0.57	0.03	10	0.15	0.08 ×10^{10}

Table 2: Chosen sites, geographical data and monthly mean values of climate data in the critical month.

Site	Geographical data	Critical month	T_e (°C)	p_{ve} (Pa)	Ψ_e (%)
Milano	Latitude 45°28'0'' Longitude 9°13'0'' Altitude 122 m	January	2.0	593.3	84
Pisa	Latitude 43°46'15'' Longitude 10°23'2'' Altitude 5 m	January	5.5	786.6	87
Agrigento	Latitude 37°14'16'' Longitude 13°38'9'' Altitude 40 m	February	7.7	813.5	77

A typical indoor room was considered, having a net floor area S=85 m^2 (approximately 8.0 m in width and 10.6 m in length) and a net volume V=230 m^3. The following mean values were assumed constant: internal air temperature (T_i=20°C) and number of air changes (n=0.5 h^{-1}). The room was assigned a humidity class of '3', i.e. buildings with unknown occupancy (see Annex B). With these assumptions, the values of internal moisture production rate (Γ_v), calculated according to [6] (see also Annex B), are indicated in Table 3.

If Glaser diagrams [6] relative to R1 and R2 roofs were drawn in the case of a non-ventilated air gap, interstitial condensation phenomena would be evidenced in both the roofs for all the chosen sites. The interstitial condensation may be avoided by applying a vapour barrier [22], but such a solution should be considered with extreme caution due to the drawbacks it could cause, which sometimes can undo the advantages expected by its use. Alternatively it could be possible to adjust the indoor ventilation air flow rate till to the value of G_0^* as calculated with Eq.(14). The results of this calculations are shown in Table 3 for the different sites in the cases of R1 and R2 roofs. However, this solution seems to be hardly feasible due to the excessively high values of ventilation air flow rates, which would be incompatible with the requirements for comfort and energy saving in buildings. To support the latter consideration, a comparison between ventilation air flow rate G_0, obtained with a fixed number of air changes (n=0.5 h^{-1}), typically suggested for hygiene and health in indoor environment [41], and those necessary to avoid interstitial condensation G_0^*, has been done in Table 3. As can be observed, the values of G_0^* are considerably greater than G_0 with increments varying from a minimum of 3 to a maximum of about 7 times, this leads to rises in ventilation heat loss (ΔQ_v) for the considered cases ranging from a minimum of 1.5 kW up to a maximum of 5.9 kW.

Table 3: Calculated values of Γ_v, G_0, n, G_0^*, n^*, ΔQ_v in the cases of R1 and R2 roofs with non-ventilated air gap.

Roof	**Site**	$\boldsymbol{\Gamma_v}$ (kg/h)	Standard values		Values to avoid interstitial condensation		$\boldsymbol{\Delta Q_v}$ (kW)
			$\mathbf{G_0}$ (m^3/h)	**n** (h^{-1})	$\mathbf{G_0^*}$ (m^3/h)	$\mathbf{n^*}$ (h^{-1})	
R1	Milano	0.65	115.0	0.5	723.0	3.1	5.0
	Pisa	0.53			729.3	3.2	4.0
	Agrigento	0.46			403.7	1.8	1.5
R2	Milano	0.65	115.0	0.5	828.5	3.6	5.9
	Pisa	0.53			832.6	3.6	4.7
	Agrigento	0.46			432.4	1.9	1.7

In order to avoid interstitial condensation, a convenient solution seems to be the ventilation of the air gap. Ventilation of tilted roofs usually occurs naturally through a chimney effect [20,30], on the contrary, in the case of flat roofs (investigated in this paper), due to their very low slope (usually less than 5%), forced ventilation will be necessary.

4- Results and discussion

The ventilation air flow rate (forced ventilation in flat roofs) was studied as a function of different parameters: geometric (i.e. thermal insulation thickness, layers' distribution with respect to the air gap), thermophysical (i.e. thermal conductivity and vapour resistance of thermal insulation, internal moisture production rate) and climate (i.e. temperature and relative humidity of the external air).

Three different thermal insulation materials (i.e. mineral wool, wood fibre, expanded polystyrene) were selected, characterized by the same thermal conductivity (k=0.038 W/mK) and by the same thickness (d_{iso}=0.12 m). The thermophysical properties of the three thermal insulation materials are shown in Table 4.

Table 4: Thermophysical properties of the selected thermal insulation materials.

ID	Thermal insulation	ρ (kg/m^3)	c_p (J/kgK)	μ	s_d (m)	r_v (m^{2}sPa/kg)
TM1	Mineral wool	135	1030	1	0.12	0.06×10^{10}
TM2	Wood fibre	55	2100	5	0.60	0.3×10^{10}
TM3	Expanded polystyrene	15	1260	30	3.60	1.8×10^{10}

Table 5: Minimum values of the volumetric air flow rate G (m^3/h) in order to avoid the interstitial condensation.

Roof		**R1**			**R2**		
Thermal insulation		**TM1**	**TM2**	**TM3**	**TM1**	**TM2**	**TM3**
$\mathbf{R_s}$ (m^{2}K/W)		0.54	0.54	0.54	0.34	0.34	0.34
$\mathbf{R_c}$ (m^{2}K/W)		3.45	3.45	3.45	3.65	3.65	3.65
$\mathbf{R_v}$ (m^{2}sPa/kg)		0.16×10^{10}	0.40×10^{10}	1.90×10^{10}	1.49×10^{10}	1.73×10^{10}	3.23×10^{10}
G (m^3/h)	**Milano**	110.6	47.7	10.4	15.6	13.5	7.3
	Pisa	83.9	36.3	7.9	12.0	10.3	5.6
	Agrigento	25.5	11.3	2.5	3.6	3.1	1.7

In Table 5 the values of the ventilation air flow rate G are shown for the ventilated air gap, as calculated using Eqs.(10), (11), (12), and (13), for R1 and R2 roofs, in the chosen sites for the selected thermal insulation materials. The air flow rate G (m^3/h) is to be considered, hereinafter, relative to the entire roof. The air flow rate values have been increased by 20% for safety reasons. The interstitial condensation phenomena are absent within the internal cladding (c), see Fig.1. The surface thermal resistances of the air gap have been evaluated according to the method discussed in previous papers [20,30]; within the considered ranges of temperature and velocity, these thermal resistances have been assumed to be constant and equal to the mean value of 0.07 m^{2}K/W. By comparison, in Table 5 are shown the values of thermal resistances R_s and R_c (m^{2}K/W) and of internal cladding vapour resistance R_v (m^{2}sPa/kg) for all the thermal insulation materials. It should be noted that the lowest possible air flow rate is desired in order to reduce energy consumption of the mechanical ventilation system (e.g. a small sized fan). From the results shown in Table 5, it is evident that R2 roof has better hygrothermal

behaviour when compared to R1 roof, due to a different distribution of the layers and their vapour resistances: the air flow rates required by R2 roof are significantly lower than those required by R1 roof. Furthermore, the effect of the climate data of the chosen sites (i.e. Milano, Pisa, Agrigento) is evident. In particular, for a given roof with a certain thermal insulation material, the ventilation air flow rates are highest in the coldest location (Milano). For both roofs and a given site, the air flow rates decrease with increasing internal cladding vapour resistance (R_v). It should be noted that in both analysed roofs the thermal insulation is placed below the air gap (toward the internal cladding, see Fig.3). The thermal loss increment (Δ) between the flat roof having a ventilated air gap and the corresponding non-ventilated roof, as calculated with Eq.(15), is lower than 5%.

All the air flow rates are quite low, easily obtainable with a small sized electrical fan suited for outdoor installation. An example of suitable fan is an axial centrifugal fan for air ducts, available in the market, with a nominal volumetric air flow rate of 80 m^3/h, a maximum static pressure head of 28 Pa and an electrical power consumption of 6 W. Using such a fan and subdividing the air gap into 4 ducts (2.0 m width, 10.6 m length and 0.10 m thickness), the minimum air flow rate for each duct is equal to a quarter of that shown in Table 5. Taking into account the pressure losses (local loss coefficients: 24 for the inlet vent, 0.8 for the protective metal mesh, 1.2 for the outlet vent) the fan is able to provide an air flow rate equal to 68 m^3/h which is greater than the minimum value required by each duct. So that, for each chosen site, a number of 4 fans can be used with an overall electrical power of 24 W. The use of a fan allows also a reduction of thermal load during the summer season, with a consequently reduction of the overheating risk for the indoor environment [27,30].

4.1- Influence of geometric parameters on ventilation air flow rate

The influence of the thickness of the thermal insulation layer on the ventilation air flow rate G is shown in Figures 4 and 5, in the case of mineral wool (TM1 material, see Tab.4). From the analytical model, it can be observed that, hygrothermal conditions being equal, an increase in the internal cladding thermal resistance (R_c) is accompanied by a reduction in the waterproofing layer temperature (T_b) and thus by an increase in air flow rate G. On the contrary, an increase in the internal cladding vapour resistance (R_v) causes a reduction in G, due to the reduction of vapour in the air gap. For a given roof, an increase in the thermal insulation thickness (d_{iso}) causes both an increase in R_c, which in turn would cause an increase in G, as well as an increase in R_v, which in turn would cause a reduction in G. According to the relative entity of these two contrasting effects, the function $G(d_{iso})$ may take on qualitatively different trends. For example for the R1 roof (see Fig.4), the air flow rates initially increase with increasing thermal insulation thickness and then decrease. For the R2 roof (see Fig.5) the air flow rates increase with increasing thermal insulation thickness; from a hygrothermal point of view, and thus regardless of the thermal insulation requirements, it is not advantageous to isolate the R2 roof. In order to comply with the requirements set by the recent Italian legislation

regarding energy performance of buildings [10], the roofs of buildings must have a maximum value of the thermal transmittance in the range of 0.23-0.38 W/m^{2}K, depending on the climate zone where the building is located. It results in a thermal insulation thicknesses variable from 8 to 16 cm. For this reason, in the case of R1 roof the use of a thermal insulation thickness higher than 8 cm determines a favourable decrease in ventilation air flow rates.

In all the analysed cases the thermal insulation is composed of a single layer located in the internal cladding (see Fig.3). It should be noted that a different layout of the insulation material may result in a considerable increase in ventilation air flow rate. Consider distributing the thermal insulation (total thickness d_{iso}) in two layers, the first layer having thickness d_s placed below the air gap and the second layer having thickness (d_{iso}–d_s) placed above the air gap. Let $z=(d_{iso}–d_s)d_{iso}^{-1}$ be the fraction of the thermal insulation located in the external cladding, with $0\leq z\leq 1$. For $z=0$, the entire thermal insulation is located below the air gap (within the internal cladding) and for $z=1$, the entire insulation is located above the air gap (within the external cladding). Figures 6 and 7 show the ventilation air flow rates G in function of the thermal insulation position for both roofs (with TM1 thermal insulation, d_{iso}=0.12 m) and for all the chosen sites. The influence of the parameter z on the air flow rates is more evident in R1 roof rather than in R2 roof. It can be quantitatively observed that the roofs having insulation placed below the air gap (z=0) require lower ventilation air flow rates compared to roofs having insulation placed above the air gap (z=1).

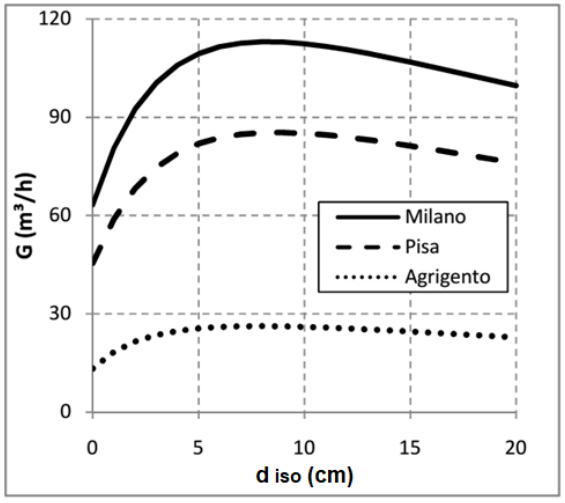

Figure 4: R1 roof (with TM1 thermal insulation), trends of the volumetric air flow rate (G) in function of the thermal insulation thickness (d) for the chosen sites.

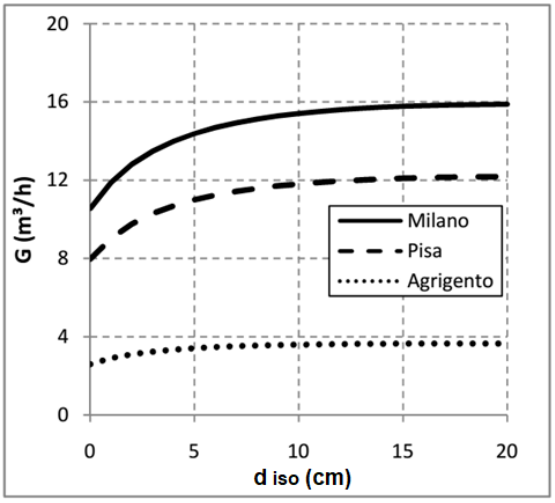

Figure 5: R2 roof (with TM1 thermal insulation), trends of the volumetric air flow rate (G) in function of the thermal insulation thickness (d) for the chosen sites.

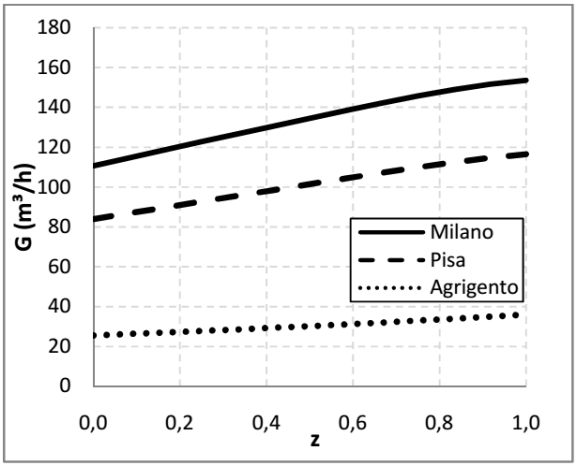

Figure 6: R1 roof (with TM1 thermal insulation, d_{iso}=0.12 m), trends of the volumetric air flow rate (G) in function of the z parameter for the chosen sites.

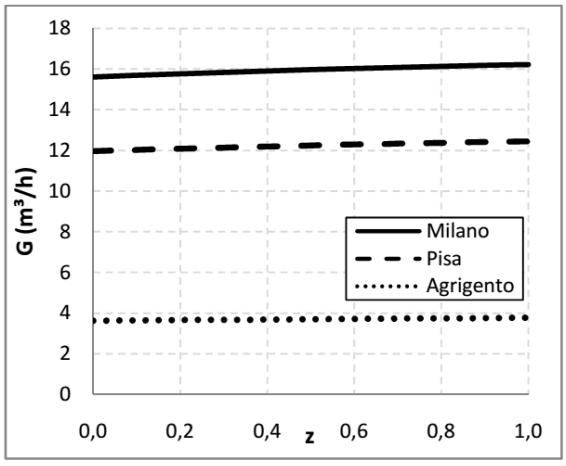

Figure 7: R2 roof (with TM1 thermal insulation, d_{iso}=0.12 m), trends of the volumetric air flow rate (G) in function of the z parameter for the chosen sites.

4.2- Influence of thermophysical parameters on ventilation air flow rate

Figure 8 shows the trends of the ventilation air flow rate G in function of the thermal conductivity k of the insulation (having fixed the water vapour resistance μ=1) for the more widespread commercially available thicknesses (8 cm, 12 cm and 16 cm), in the case of R1 roof, with z=0, located in Milano. The ventilation air flow rates decrease with increasing the thermal conductivity of the insulation. Let k be the thermal conductivity of a given insulation with increasing insulation thickness d_{iso} the ventilation air flow rates decrease. For example, from the Fig.8, if a fan capable of producing an air flow rate G=110 m^3/h is chosen, the following combinations of thermal conductivity and thickness can be used: k=0.032 W/mK and d_{iso}=8 cm; k=0.039 W/mK and d_{iso}=12 cm; k=0.042 W/mK and d_{iso}=16 cm.

Figure 9 shows the trends of the ventilation air flow rate G in function of the water vapour resistance factor μ of the thermal insulation (having fixed the thermal conductivity k=0.038 W/mK), in the same case of Fig.8. Given an insulation thickness, the ventilation air flow rates decrease with an increase in the vapour resistance factor and thus with an increase in vapour resistance of the internal cladding. Water vapour resistance factor μ being equal, with increasing thermal insulation thicknesses there is a decrease in ventilation air flow rates. For example, from the Fig.9, if a fan capable of producing an air flow rate G=40 m^3/h is chosen, the following combinations of thickness and water vapour resistance factor can be used: d_{iso}=16 cm and μ=5.5; d_{iso}=12 cm and μ=6.5; d_{iso}=8 cm and μ=8.5.

The same qualitative effects of k and μ on G, as shown respectively in Figs.8 and 9 for R1 roof, can be observed also in the case of R2 roof.

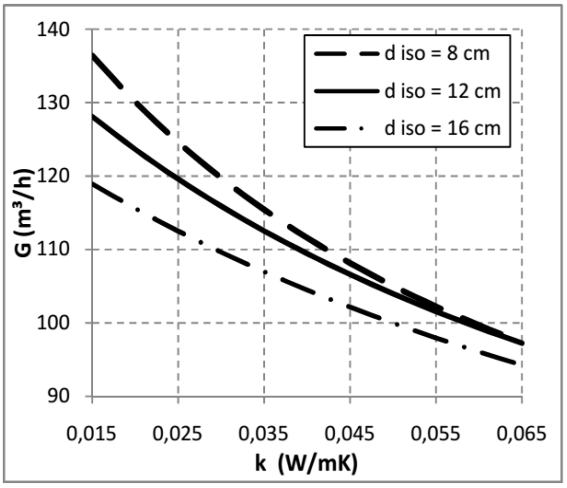

Figure 8: Trends of the volumetric air flow rate (G) for the R1 roof (z=0) located in Milano in function of the thermal conductivity (k) of the insulation material (with μ=1) for different values of the insulation layer thickness (d_{iso}).

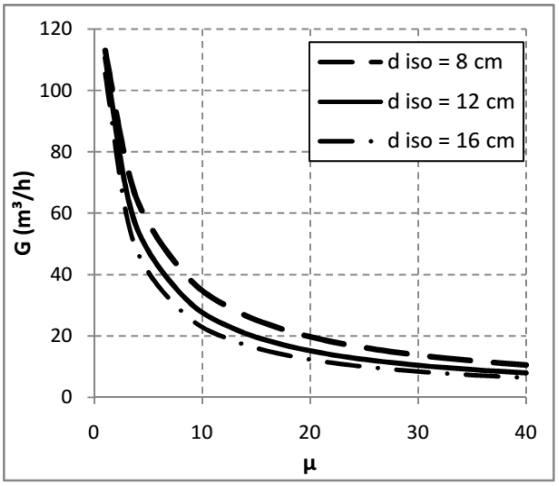

Figure 9: Trends of the volumetric air flow rate (G) for the R1 roof (z=0) located in Milano in function of the water vapour resistance factor (μ) of the insulation material (with k=0.038 W/mK) for different values of the insulation layer thickness (d_{iso}).

4.3- Influence of climate parameters on ventilation air flow rate

In Figure 10 are shown the trends of the ventilation air flow rate G in function of the external air temperature T_e (°C) for different solutions of R1 roof (R1 with TM1, R1a with TM2 and R1b with TM3, see Tab.4), for R2 roof and for different values of external air relative humidity Ψ_e (with Γ_v=0.5 kg/h). Obviously, with an increase in external air temperature the values of air flow rate rapidly decrease. From Fig.10, T_e being equal, for R1 roof with a decrease in external air relative humidity, the values of air flow rate decrease; for example, with a given T_e and Ψ_e=90%, the required ventilation air flow rate is approximately double than the air flow rate required with Ψ_e=80%. Dependency from external air relative humidity is less evident for R2 and R1b roofs, as they require lower air flow rates.

In Figure 11 are shown the trends of the ventilation air flow rate G in function of the external air relative humidity Ψ_e (with T_e=0°C and Γ_v=0.5 kg/h) for the different solutions of R1 roof (R1, R1a and R1b) and for R2 roof. The ventilation air flow rates increase with increasing the external air relative humidity. From Fig.11, Ψ_e being equal, for the three different solutions of R1 roof, with an increase in water vapour resistance factor (μ=1 for R1, μ=5 for R1a, μ=30 for R1b) there is a decrease in ventilation air flow rates; in fact R1b solution shows a better hygrothermal behaviour than the other solutions (R1 and R1a), R1b solution also requires lower ventilation air flow rates than R2 roof.

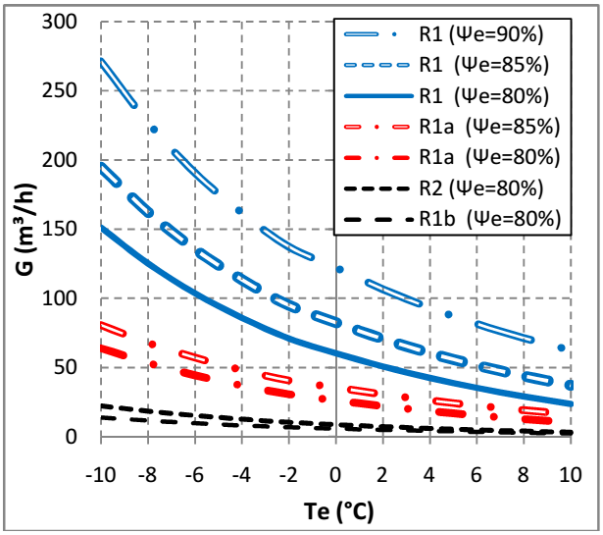

Figure 10: Trends of the volumetric air flow rate (G) in function of the external air temperature (T_e) for different roofs and for different values of relative humidity (Ψ_e), with Γ_v=0.5 kg/h.

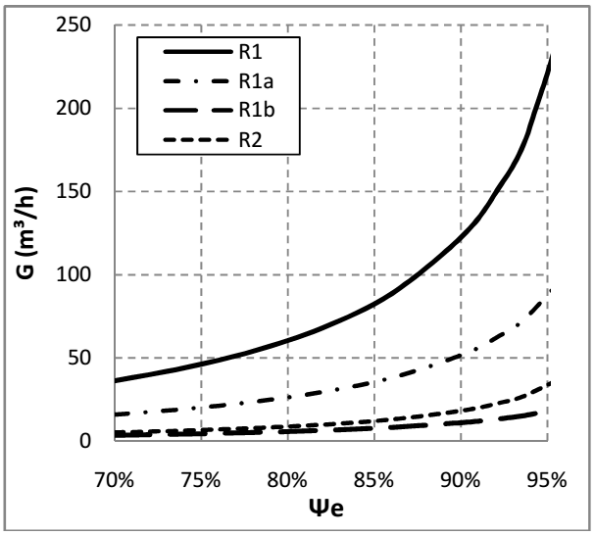

Figure 11: Trends of the volumetric air flow rate (G) in function of the external air relative humidity (Ψ_e) for different roofs, with T_e=0°C, Γ_v=0.5 kg/h.

5. Concluding remarks and future developments

Among the components of the building envelope, the flat roof, due to the inevitable presence of a waterproofing layer that constitutes a barrier to the water vapour diffusion, is one of the most prone to the interstitial condensation phenomena. These phenomena can be avoided with the use of vapour retarders, appropriately positioned within the roof stratigraphy. This solution, although in some cases could be the most economically advantageous, is not the only one. Alternatively, forced ventilation of suitable air gaps can be applied. The designer must, therefore, have some tools to choose the desired solution case by case, based on techno-economic analysis.

In this paper an analytical model, useful to assessing the ventilation air flow rate necessary to avoid interstitial condensation, has been developed and described. The analytical model has been applied to two study cases of flat roofs widespread in Italy. The ventilation air flow rate has been quantitatively studied as a function of:

- geometrical parameters (thickness of the thermal insulation and fraction of the thermal insulation located in the external cladding), considering three sites representative of three different Italian climate zones;
- thermophysical parameters (thermal conductivity, water vapour resistance factor and internal moisture production rate), considering the coldest chosen site;
- climate parameters (temperature and humidity of the external air).

From the results of the conducted analysis, it has been shown that the ventilation air flow rates, calculated using the analytical model, are always rather modest and easily realized by the use of small size fans with very low energy consumptions. The increase in thermal heat losses of the ventilated flat roof with respect to the non-ventilated structure is less than 5%. Moreover it has been possible to

highlighting the different hygrothermal behaviours of the analysed roofs. As general remark, it can be pointed out that the technical solution of the ventilated flat roof with the air gap positioned above the load bearing structure of the roof (R2 roof) requires significantly lower air flow rate than the solution with the air gap positioned below the load bearing structure of the roof (R1 roof). Obviously, in order to minimize the ventilation air flow rates, it is advisable to use a thermal insulation with a high water vapour resistance factor (μ) to reduce the amount of vapour in the air gap, for example the replacement of a thermal insulation characterized by μ=10 with one characterized by μ=40 allows a reduction of about 50% of the ventilation air flow rates for all the analysed conditions. In order to realize zero energy buildings, the electricity consumption of the fans (necessary for the ventilation of the flat roof), though low, should be taken into account in the annual energy balance of the building. Obviously to minimize the electrical energy consumption of the fans, ventilation air flow rate control logics could be implemented, based on the results shown in this paper and by measuring the climate parameters (temperature and relative humidity of the external air) and the internal moisture production rate. This may be of particular interest in buildings with a large roof extension, as usually occurs for example in commercial and school buildings.

Although the model is based on well-known equations of the heat and moisture transfer, it does not take into account variable climatic conditions, for example day-night cycles or seasonal cycles. For these cases, dynamic calculation methods are needed. The use of average monthly conditions, which characterizes the developed model, is typical of simplified methods aimed to make preliminary selections of technical solutions. As future developments of this study it could be interesting to compare the results with those obtained, as soon as available in the literature, from experimental measurements or from CFD analysis of this particular type of roofs.

References

[1] Zirkelbach, D., Mehra, S.R., Sedlbauer, K.P., Kunzel, H.M., Stockl, B., A hygrothermal green roof model to simulate moisture and energy performance of building components, (2017) Energy and Buildings, 145, pp.79-91. DOI: 10.1016/j.enbuild.2017.04.001

[2] Stanek, K., Tywoniak, J., Richter, J., Bureö, M., Kopeck, P., Volf, M., Studies on hygrothermal performance of wood elements in building constructions-remarks on methodology, (2016) Wood Research, 61(4), pp.637-650

[3] Moradias, P.A., Silva, P.D., Castro-Gomes, J.P., Salazar, M.V., Pires, L., Experimental study on hygrothermal behaviour of retrofit solutions applied to old building walls, (2012) Construction and Building Materials, 35, pp.864-873. DOI: 10.1016/j.conbuildmat.2012.04.138

[4] Bellia, L., Minichiello, F., A simple evaluator of building envelope moisture condensation according to an European Standard, (2003) Building and Environment, 38(3), pp.457-468. DOI: 10.1016/S0360-1323(02)00060-4

[5] Barsottelli, M., Cellai, G.F., Fratini, F., Manganelli Del Fà, C., The hygrometric behaviour of some artificial stone materials used as elements of masonry walls, (2001) Materials and Structures/Materiaux et Constructions, 34(238), pp.211-216.

[6] European Committee for Standardization, EN ISO 13788: Hygrothermal performance of building components and building elements - Internal surface temperature to avoid critical surface humidity and interstitial condensation - Calculation methods, Brussels, Belgium, 2012.

[7] European Committee for Standardization, EN 15026: Hygrothermal performance of building components and building elements - Assessment of moisture transfer by numerical simulation, Brussels, Belgium, 2007.

[8] European Union, Directive 2002/91/CE of the European Parliament and of the Council of 19/12/2002 on the energy performance of buildings, Off. J. Eur. Union. http://eur-lex.europa.eu/legal-content/EN/TXT/?qid=1500284297674&uri=CELEX:32002L0091 (accessed on 20/07/2018).

[9] European Union, Directive 2010/31/EU of the European Parliament and of the Council of 19/05/2010 on the energy performance of buildings (recast), Off. J. Eur. Union. http://eur-lex.europa.eu/legal-content/EN/TXT/?qid=1500284414386&uri=CELEX:32010L0031 (accessed on 20/07/2018).

[10] Italian Governement, Ministry of Economic Development, Applicazione delle Metodologie di Calcolo delle Prestazioni Energetiche e Definizione delle Prescrizioni e dei Requisiti Minimi degli Edifici; Ministry Decree 26/06/2015, Rome, Italy, 2015. (*In Italian*). http://www.gazzettaufficiale.it/eli/id/2015/07/15/15A05198/sg (accessed on 20/07/2018).

[11] Italian Governement, President of the Italian Repubblic, Regolamento di attuazione dell'articolo 4, comma 1, lettere a) e b), del decreto legislativo 19 agosto 2005, n. 192, concernente attuazione della direttiva 2002/91/CE sul rendimento energetico in edilizia; Presidential Decree n. 59 02/04/2009, Rome, Italy, 2009. (*In Italian*). http://www.gazzettaufficiale.it/eli/id/2009/06/10/009G0068/sg (accessed on 20/07/2018)

[12] Bluyssen P.M., Towards an integrative approach of improving indoor air quality, (2009) Building and Environment, 44(9), pp.1980-1989. DOI: 10.1016/j.buildenv.2009.01.012

[13] Wei S., Jones R., de Wilde P., Driving factors for occupant-controlled space heating in residential buildings, (2014) Energy and Building, 70, pp.36-44. DOI: 10.1016/j.enbuild.2013.11.001

[14] Mumovic, D., Ridley, I., Oreszczyn, T., Davies, M., Condensation risk: Comparison of steady-state and transient methods, (2006) Building Services Engineering Research and Technology, 27 (3), pp. 219-233. DOI: 10.1191/0143624406bse163oa

[15] Leccese, F., Salvadori, G., Asdrubali, F, Gori, P., Passive thermal behaviour of buildings: Performance of external multi-layered walls and influence of internal walls, (2018) Applied Energy, 225, pp. 1078-1089. DOI: 10.1016/j.apenergy.2018.05.090

[16] Pepe D., Rossetti M., Antoniol E., Covre V., Measurement of residential buildings using the "Blower door test" and its relation with indoor air quality, (2016) Proceedings of the CIB World Building Congress 2016 (Tampere University of Technology), pp.669-679. ISBN: 978-952-15-3744-8

[17] Alchapar, N.L., Correa, E.N., Aging of roof coatings. Solar reflectance stability according to their morphological characteristics, (2016) Construction and Building Materials, 102, pp.297-305. DOI: 10.1016/j.conbuildmat.2015.11.005

[18] Bortoloni, M., Bottarelli, M., Piva, S., Summer Thermal Performance of Ventilated Roofs with Tiled Coverings, (2017) Journal of Physics: Conference Series, 796 (1), Art.n.012023. DOI: 10.1088/1742-6596/796/1/012023

[19] D'Orazio, M., Di Perna, C., Principi, P., Stazi, A., Effects of roof tile permeability on the thermal performance of ventilated roofs: Analysis of annual performance, (2008) Energy and Buildings, 40(5), pp.911-916. DOI: 10.1016/j.enbuild.2007.07.003

[20] Ciampi, M., Leccese, F., Tuoni, G., Energy analysis of ventilated and microventilated roofs, (2005) Solar Energy, 79(2), pp.183-192. DOI: 10.1016/j.solener.2004.08.014

[21] Walter, A., de Brito, J., Grandao Lopes, J., Current flat roof bituminous membranes waterproofing systems - inspection, diagnosis and pathology classification, (2005) Construction and Building Materials, 19, pp.233-242. DOI: 10.1016/j.conbuildmat.2004.05.008

[22] Gutt G.S., Condensation in Attics: Are vapour barriers really the answer?, (1979) Energy and Buildings, 2(4), pp.251-258. DOI: 10.1016/0378-7788(79)90036-7

[23] Zhang, T., Tan, Y., Yang, H., Zhang, X., The application of air layers in building envelopes: A review, (2016) Applied Energy, 165, pp.707-734. DOI: 10.1016/j.apenergy.2015.12.108

[24] Sadineni, S.B., Madala, S., Boehm, R.F., Passive building energy savings: A review of building envelope components, (2011) Renewable and Sustainable Energy Reviews, 15(8), pp.3617-3631. DOI: 10.1016/j.rser.2011.07.014

[25] Bianco, V., Diana, A., Manca, O., Nardini, S., Thermal behaviour evaluation of ventilated roof under variable solar radiation, (2016) International Journal of Heat and Technology, 34 (Special Issue 2), pp.S346-S350. DOI: 10.18280/ijht.34S222

[26] Gagliano, A., Patania, F., Nocera, F., Ferlito, A., Galesi, A., Thermal performance of ventilated roofs during summer period, (2012) Energy and Buildings, 49, pp.611-618. DOI: 10.1016/j.enbuild.2012.03.007

[27] Ciampi, M., Leccese, F., Tuoni, G., Cooling of buildings: Energy efficiency improvement through ventilated structures, (2003) Sustainable World, 7, pp.199-210.

[28] Gagliano, A., Nocera, F., Aneli, S., Thermodynamic analysis of ventilated façades under different wind conditions in summer period, (2016) Energy and Buildings, 122, pp.131-139. DOI: 10.1016/j.enbuild.2016.04.035

[29] Charde, M., Gupta, R., Effect of energy efficient building elements on summer cooling of buildings, (2013) Energy and Buildings, 67, pp.616-623. DOI: 10.1016/j.enbuild.2013.08.054

[30] Ciampi, M., Leccese, F., Tuoni, G., Ventilated facades energy performance in summer cooling of buildings, (2003) Solar Energy, 75(6), pp.491-502. DOI: 10.1016/j.solener.2003.09.010

[31] Kimouche, N., Mahri, Z., Abidi-Saad, A., Popa, C., Polidori, G., Maalouf, C., Effect of inclination angle of the adiabatic wall in asymmetrically heated channel on natural convection: Application to double-skin façade design, (2017) Journal of Building Engineering, 12, pp.171-177. DOI: 10.1016/j.jobe.2017.06.002

[32] Elarga, H., De Carli, M., Zarrella, A., A simplified mathematical model for transient simulation of thermal performance and energy assessment for active facades, (2015) Energy and Buildings, 104, art. no. 5988, pp. 97-107. DOI: 10.1016/j.enbuild.2015.07.007

[33] D'Orazio, M., Perna, C.D., Stazi, F., Thermal behaviour of vented roofs, (2009) Structural Survey, 27(5), pp.411-422. DOI: 10.1108/02630800911002657

[34] Li, D., Zheng, Y., Liu, C., Qi, H., Liu, X., Numerical analysis on thermal performance of naturally ventilated roofs with different influencing parameters, (2016) Sustainable Cities and Society, 22, pp. 86-93. DOI: 10.1016/j.scs.2016.02.004

[35] Tian, Y., Bai, X., Qi, B., Sun, L., Study on heat fluxes of green roofs based on an improved heat and mass transfer model, (2017) Energy and Buildings, 152, pp. 175-184. DOI: 10.1016/j.enbuild.2017.07.021

[36] Zingre, K.T., Yang, E.-H., Wan, M.P., Dynamic thermal performance of inclined double-skin roof: Modelling and experimental investigation, (2017) Energy, 133, pp.900-912. DOI: 10.1016/j.energy.2017.05.181

[37] Tong, S., Li, H., An efficient model development and experimental study for the heat transfer in naturally ventilated inclined roofs, (2014) Building and Environment, 81, pp.296-308. DOI: 10.1016/j.buildenv.2014.07.009

[38] Susanti, L., Homma, H., Matsumoto, H., Suzuki, Y., Shimizu, M., A laboratory experiment on natural ventilation through a roof cavity for reduction of solar heat gain, (2008) Energy and Buildings, 40(12), pp.2196-2206. DOI: 10.1016/j.enbuild.2008.06.016

[39] Ghazi Wakili, K., Frank, Th., A humidity dependent vapour retarder in non-ventilated flat roofs. In situ measurements and numerical analysis, (2004) Indoor and Built Environment, 13(6), pp.433-441. DOI: 10.1177/1420326X05047376

[40] European Committee for Standardization, EN ISO 6946: Building components and building elements – Thermal resistance and thermal transmittance – Calculation method, Brussels, Belgium, 2017.

[41] European Committee for Standardization, EN ISO 52016-1: Energy performance of buildings – Energy needs for heating and cooling, internal temperatures and sensible and latent heat loads – Part 1: Calculation procedures, Brussels, Belgium, 2017.

[42] Italian Committee for Standardization (UNI), UNI 10349-1: Riscaldamento e raffrescamento degli edifici – Dati climatici – Parte 1: Medie mensili per la valutazione della prestazione termo-energetica dell'edificio e metodi per ripartire l'irradianza solare nella frazione diretta e diffusa e per calcolare l'irradianza solare su di una superficie inclinata (*in Italian*), Milano, Italy, 2016.

[43] Italian Committee for Standardization (UNI), UNI/TS 11300-1: Prestazioni energetiche degli edifici – Parte 1: Determinazione del fabbisogno di energia termica dell'edificio per la climatizzazione estiva ed invernale (*in Italian*), Milano, Italy, 2014.

ANNEX A – Definitions of Italian climate zones and critical months

The Italian territory is divided into 6 climate zones (named from A to F) according to the number of heating degree-days (GG) and regardless of geographical location, as shown in Table A1 [10]. A low GG value indicates that the external air temperatures are very close to the conventionally set temperature for the heated spaces (20 °C) and therefore the climate is not very rigid (e.g. climate zone A, for example in the case of South Italy islands). A high GG value, on the contrary, indicates that the external air temperatures are often very lower than 20 °C and the climate is therefore rigid (e.g. climate zone F, for example in the case of sites on the mountains of Northern Italy). The conventional periods of the year for which the heating systems are switched on and the conventional daily usage times are established in function of the climate zone [10,43]. For example, in the case of the climate

zone D, the most widespread in Italy, heating systems can be activated from 1 November to 15 April for up to 12 hours a day. The outdoor environment climate data has been recently updated by Italian Committee for Standardization [42]. In [42] the climate data of 110 meteorological stations, distributed on the national territory, are reported; among these, a percentage of 99% belongs to the climate zones C, D and E.

Table A1: Definition of Italian climate zones.

GG	Climate zone
≤ 600	A
600 < GG ≤ 900	B
900 < GG ≤ 1400	C
1400 < GG ≤ 2100	D
2100 < GG ≤ 3000	E
GG > 3000	F

Based on the climate data of each site, in relation to the interstitial condensation, can be defined 'critical month' the month that shows the most unfavourable combination of monthly mean values of water vapour pressure (p_{ve}) and temperature (T_e) of the external air. In Italy, the critical month occurs in the heating period and, generally, it may vary from December to February. In relation to the surface condensation, the 'critical month' can be assumed as the month with the highest required value of temperature factor at the internal surface (f), defined as follows:

$$f = (T_{si} - T_e)(T_i - T_e)^{-1} \quad \text{(A1)}$$

with: T_i internal operative air temperature (e.g. T_i=20°C, during the heating period, according to the Italian national legislation [10]), T_e external air temperature (e.g. monthly mean values, extracted from standard climate data [42]), T_{si} the minimum acceptable value of temperature of the internal surface (e.g. to avoid critical surface humidity [6]).

ANNEX B – Evaluation of internal moisture production rate

The recent technical Standard on the hygrothermal performance of building components and building elements [6] identifies five internal humidity classes in function of the building use, as indicated in Table B1.

Table B1: Internal humidity classes in function of the building use.

Humidity class	Building use
1	Unoccupied buildings, storage of dry goods
2	Offices, dwellings with normal occupancy and ventilation
3	Buildings with unknown occupancy
4	Sports halls, kitchens, canteens
5	Special buildings, e.g. laundry, brewery, swimming pool

Assigned the humidity class to the building, it is possible to evaluate the difference between internal and external water vapour pressure (Δp) in function of the external air temperature (T_e) by using the graph of Figure B1.

Using a constant number of air changes [6], Δp can be expressed in function of the internal moisture excess (Δv, kg/m^3) through the following equation [4,6]:

$$\Delta p = \Delta v \Re_v \left(\frac{T_i + T_e}{2}\right) = \frac{\Gamma_v}{nV} \Re_v \left(\frac{T_i + T_e}{2}\right) \quad \text{(B1)}$$

whit: $\Re_v$ the gas constant for water ($\Re_v$=462 m^{3}Pa/kgK); T_i and T_e internal and external air temperature respectively (K); n number of air changes (h^{-1}); Γ_v internal moisture production rate (kg/h); V net volume of the room (m^3).

From Eq.(B1) the value of Γ_v can be calculated as follows (n=0.5 h^{-1}):

$$\Gamma_v = 0.0022\, \Delta p V (T_i + T_e)^{-1} \quad \text{(B2)}$$

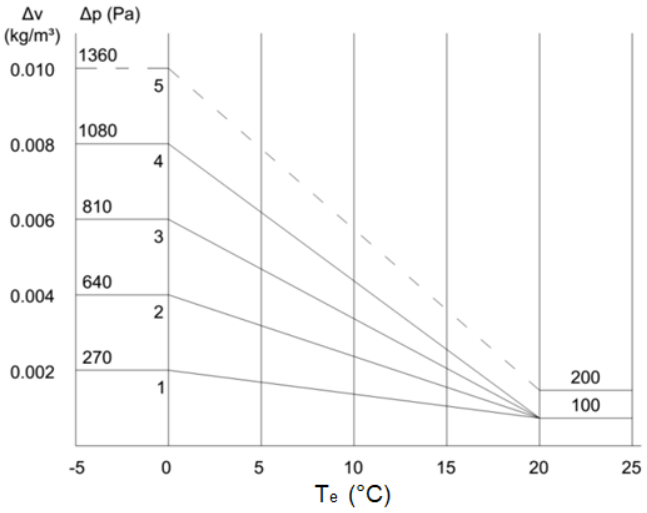

Figure B1: Trends of Δp in function of the external air temperature T_e for the different humidity classes.